



## Characterization of thermal desorption instrumentation with a direct liquid deposition calibration method for trace 2,4,6-trinitrotoluene quantitation

Christopher R. Field<sup>a,\*</sup>, Braden C. Giordano<sup>a</sup>, Duane A. Rogers<sup>a</sup>, Adam L. Lubrano<sup>b</sup>, Susan L. Rose-Pehrsson<sup>a</sup>

<sup>a</sup> Chemistry Division, USA Naval Research Laboratory, Washington, DC 20375, USA

<sup>b</sup> Nova Research, Inc., Alexandria, VA 22308, USA

### ARTICLE INFO

#### Article history:

Received 10 November 2011

Received in revised form

19 December 2011

Accepted 20 December 2011

Available online 8 January 2012

#### Keywords:

Explosives

GC-ECD

Quantitation

2,4,6-Trinitrotoluene (TNT)

Thermal desorption

Cryo-focusing

### ABSTRACT

The use of thermal desorption systems for the analysis of trace vapors typically requires establishing a calibration curve from vapors generated with a permeation tube. The slow equilibration time of permeation tubes causes such an approach to become laborious when covering a wide dynamic range. Furthermore, many analytes of interest, such as explosives, are not available as permeation tubes. A method for easily and effectively establishing calibration curves for explosive vapor samples via direct deposition of standard solutions on thermal desorption tubes was investigated. The various components of the thermal desorption system were compared to a standard split/splitless inlet. Calibration curves using the direct liquid deposition method with a thermal desorption unit coupled to a cryo-focusing inlet were compared to a standard split/splitless inlet, and a statistical difference was observed but does not eliminate or deter the use of the direct liquid deposition method for obtaining quantitative results for explosive vapors.

Published by Elsevier B.V.

### 1. Introduction

A wide range of technologies have been established and researched for vapor detection of 2,4,6-trinitrotoluene (TNT) and other explosives, namely ion mobility spectroscopy, surface acoustic wave devices, spectroscopy-based instruments, and nanostructure-based sensors [1–8]. However, Gas Chromatography (GC) with an Electron Capture Detector (ECD) or Mass Spectrometer (MS) remains the primary method for trace explosive analysis [9–20]. Previous work with thermal desorption coupled to GC-ECD/MS has been limited, and focused mainly on sampling methodology and collection efficiencies [9,10,12,17–19]. Proof-of-principle work has previously demonstrated the utility of thermal desorption with a cooled injection system (CIS) coupled to a GC-ECD/MS for detection of trace explosives [15–17]. Nanogram to picogram detection limits have been demonstrated with these prototype thermal desorption systems (TDSs) coupled to a GC-ECD/MS [11,16]. Today, commercialized TDS–CIS–GC-ECD/MS is available, making it more readily accessible for routine trace explosive detection. Manufacturers of TDS–CIS instrumentation provide recommendations and methods for atmospheric

sampling and hydrocarbon analysis, but not specifically for explosive vapors.

Method development for explosive residue and particle detection has been favored in the literature over vapor detection due in part to a lack of reliable vapor standards. Because of the low vapor pressure and rapid decomposition of these analytes, there are currently no commercially available vapor standards for nitroaromatic or nitramine explosives and no standardized method for generating explosive vapors. Consequently, quantitation is performed using calibration curves generated from liquid injections into the standard split/splitless inlet. Unfortunately, such an approach does not account for losses associated with the CIS, TDS, or sample tube sorbent. These losses lead to significant error associated with vapor concentration. Therefore, a procedure is needed for establishing calibration curves using commercially available standard solutions and to account for the variation and losses with each component in the TDS–CIS–GC-ECD/MS instrumentation.

In this work, direct deposition of a standard solution onto TDS sample tubes is investigated as a means for eventual quantitation of TNT vapor. The focus is on understanding the influence of specific instrument parameters in the detection and quantitation of TNT and the validity of the direct liquid deposition method. Specifically, the goal is to determine the losses, if any, associated with individual components of the TDS–CIS approach when compared to a conventional split/splitless GC inlet. The use of

\* Corresponding author. Tel.: +1 202 404 3365.

E-mail address: [christopher.field@nrl.navy.mil](mailto:christopher.field@nrl.navy.mil) (C.R. Field).

3,4-dinitrotoluene (3,4-DNT) as an internal standard is evaluated for TNT vapor analysis. The optimized method for a TDS–CIS–GC–ECD system established in this work could be extended to other explosives, such as cyclotrimethylenetrinitramine (RDX) and pentaerythritol tetranitrate (PETN).

## 2. Experimental

### 2.1. Apparatus

All samples were analyzed with an Agilent 7890A gas chromatograph equipped with a  $\mu$ ECD (Agilent Technologies, Santa Clara, CA, USA). For liquid samples, an Agilent 7693A Automatic Liquid Sampler was used. The performance of a baffled (or torturous path) deactivated glass liner (part No. 5181-3316; Agilent Technologies) and a baffled Siltek<sup>TM</sup>-coated glass liner (part No. 20800-214; Restek Corp., Bellefonte, PA, USA) were compared in the standard split/splitless inlet, located in the front GC inlet position. A cryogenically cooled inlet system (part No. CIS-4; GERSTEL GmbH & Co. KG, Mülheim an der Ruhr, Germany) was installed in the back inlet position of the GC. For cryo-focusing with the CIS, the inlet temperature was ramped from the initial temperature (either  $-50^{\circ}\text{C}$ ,  $0^{\circ}\text{C}$ , and  $50^{\circ}\text{C}$ ) to  $250^{\circ}\text{C}$  at  $12^{\circ}\text{C s}^{-1}$ . Similar to the split/splitless front inlet, deactivated and Siltek<sup>TM</sup>-coated glass liners were evaluated (part No. 013148-000-00 and part No. 014652-005-00, respectively; GERSTEL GmbH & Co. KG).

The CIS was operated in three separate modes: split, splitless, and solvent vent. In split mode, the split ratio was varied from 1:10 to 1:100. To match split-mode flow rates in solvent-vent mode, flow rate was varied from  $50\text{ mL min}^{-1}$  to  $550\text{ mL min}^{-1}$  with solvent-vent times from 0.0 to 4.0 min. Two C-18 split vent traps were placed in-line with the exhaust and split vent of the CIS to protect the pneumatics and valves from degradation due to acetonitrile. A septum-less head (SLH; GERSTEL GmbH & Co. KG) was provided for liquid injections onto the CIS in the absence of the TDS. The gas chromatograph was fitted with a 15-m RTX-5MS column with a 0.25-mm inner diameter and 250 nm film thickness (5% phenyl polycarborane siloxane, part No. 12620; Restek Corp., Bellefonte, PA, USA). A helium carrier column flow rate of  $5.5\text{ mL min}^{-1}$  was used for separation, and a  $\mu$ ECD auxiliary flow rate of ultra high purity nitrogen was set at  $60\text{ mL min}^{-1}$  at  $275^{\circ}\text{C}$  operating temperature.

After running liquid samples with the SLH, the TDS (part No. TDS-3; GERSTEL GmbH & Co. KG, Mülheim an der Ruhr, Germany) was coupled to the CIS and commercially available vapor sampling tubes, both with sorbent (Tenax<sup>®</sup> 60/80, part No. 009947-000-00; GERSTEL GmbH & Co. KG) and without (part No. 010650-000-00), were tested. Sample trapped on a vapor sampling tube was desorbed in the TDS and passed through a heated transfer line to the CIS where it was preconcentrated and subsequently desorbed onto the GC column. The TDS temperature was held constant at  $25^{\circ}\text{C}$  for tube insertion before being ramped at  $40^{\circ}\text{C min}^{-1}$  to  $250^{\circ}\text{C}$  to desorb trapped analyte. The helium flow rate through the TDS during desorption was evaluated from  $50$  to  $550\text{ mL min}^{-1}$ . A heated ( $300^{\circ}\text{C}$ ) deactivated stainless steel transfer line (0.74 mm OD, part No. 010963-005-00; GERSTEL GmbH & Co. KG) connected the TDS to the CIS.

### 2.2. Reagents

Analytical standards for 3,4-DNT (CAS No. 610-39-9) and TNT (CAS No. 118-96-7) were purchased from AccuStandard Inc. (New Haven, CT, USA). The internal standard used in this work was 3,4-DNT because it has similar composition to TNT but is

**Table 1**

Solutions of TNT and 3,4-DNT used for optimizing conditions for detecting trace amounts of TNT vapor. Solution 10 was injected at  $0.1\ \mu\text{L}$  with a  $0.5\ \mu\text{L}$  syringe in splitless mode. Analyte concentrations were prepared so that the same amount of mass was injected and detected for each set of conditions with the GC-ECD.

Solution	TNT ( $\text{ng}\ \mu\text{L}^{-1}$ )	3,4-DNT ( $\text{ng}\ \mu\text{L}^{-1}$ )	Split	Flow rate ( $\text{mL min}^{-1}$ )
1	5	5	0	5.59
2	5	5	1:10	61.49
3	10	10	1:20	117.39
4	15	15	1:30	173.28
5	20	20	1:40	229.18
6	25	25	1:50	285.08
7	30	30	1:60	340.98
8	35	35	1:70	396.88
9	40	40	1:80	452.77
10	45	45	1:90	508.67
11	50	50	1:100	564.57

not a degradation product of TNT. Table 1 lists the solutions prepared for each experiment and related injection concentrations produced from serial dilution of analytical standards in acetonitrile (CAS No. 75-05-8, Sigma–Aldrich, St. Louis, MO, USA).

### 2.3. Procedure

A  $1\ \mu\text{L}$  aliquot was injected from a  $10\ \mu\text{L}$  syringe (back inlet: part No. 002810, front inlet: part No. 002821; SGE Analytical Science, Victoria, Australia) into either the front or back inlet held at a constant  $250^{\circ}\text{C}$  for GC liquid injections when operating in split or solvent vent modes. A  $0.5\ \mu\text{L}$  syringe (back inlet: part No. 000410, front inlet: part No. 000415; SGE Analytical Science) was used to provide a  $0.1\ \mu\text{L}$  injection volume for splitless mode with both the front and back inlet. Because the SLH could not accommodate a tapered syringe needle, different syringes were employed for the two inlets.

After each injection, the GC oven was held constant at  $40^{\circ}\text{C}$  for 2.0 min then ramped at  $40^{\circ}\text{C min}^{-1}$  to  $210^{\circ}\text{C}$  where the temperature was held for 1.0 min, followed by a second ramp at  $40^{\circ}\text{C min}^{-1}$  to  $250^{\circ}\text{C}$  where it was held for 1.0 min. A blank acetonitrile injection was carried out before and after each 3,4-DNT/TNT sample injection.

For the purpose of GC method development,  $5\ \mu\text{L}$  of internal standard and analyte mixture was deposited onto the inside wall of the vapor sampling tube with a micropipette, and the solvent was allowed to evaporate for at least 20 min. The internal standard mixture consisted of 3,4-DNT at a concentration of  $0.1\ \text{ng}\ \mu\text{L}^{-1}$  and the concentration of TNT was varied to provide the desired quantity of TNT in each analysis. A vapor sampling tube was then inserted into the TDS and the TDS–CIS–GC sequence was initiated. To desorb analyte from a vapor sampling tube, the TDS was ramped from an initial temperature of  $25^{\circ}\text{C}$  to  $250^{\circ}\text{C}$  at  $40^{\circ}\text{C min}^{-1}$  with a final hold time of 2.0 min. Vapor from the tubes then flowed from the TDS to the CIS, where, following an initial 2.0 min hold time at  $0^{\circ}\text{C}$ , the temperature was ramped at  $12^{\circ}\text{C s}^{-1}$  to  $250^{\circ}\text{C}$ . After cryo-focusing, vapor was passed into the GC column and separated with the same GC method that was used for liquid injections. Fig. 1 graphically summarizes the methods as timing diagrams for the injection of liquid samples using only a CIS (Fig. 1A) and injection of vapor samples using sample tubes and a TDS (Fig. 1B). Only two peaks were observed in the chromatograms at 4.2 and 4.6 min corresponding to 3,4-DNT and TNT, respectively.

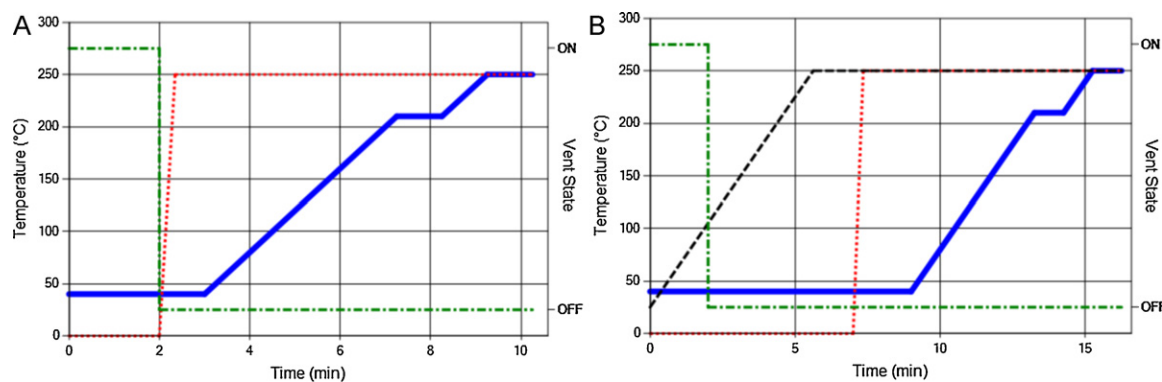


**Fig. 1.** Timing diagrams for the TDS-CIS-GC temperature ramps and vent state for (A) a CIS injection with no TDS using a septa-less head and (B) a TDS injection using sample tubes. The solvent vent mode was used for both types of injections (solid, blue, GC oven temperature; dash-dot, green, CIS temperature; dot, red, vent state; dash, black, TDS temperature). (For interpretation of the references to color in this figure legend, the reader is referred to the web version of the article.)

### 3. Results and discussion

#### 3.1. 3,4-DNT internal standard and inlet liner treatment

Previous investigations of TNT using thermal desorption have utilized 1,3-dinitronaphthalene and 3,4-DNT as an internal standard [1,12,16–18,20]. Ideally, an internal standard and analyte would have similar structures and physical properties, but can be readily separated and detected. To quantify TNT vapor by thermal desorption an internal standard should also behave thermally similar to the analyte of interest (e.g. boiling and freezing points). Prior to instrumentation characterization, 3,4-DNT was investigated as an internal standard since it has a similar structure to TNT, is not a degradation product, and can be easily separated and detected using standard methods (EPA Methods 529, 8091, 8095) [21–23]. Fig. 2A shows the peak areas for 3,4-DNT and TNT at various inlet flow rates (i.e. split ratios) for a standard GC inlet (250 °C) with a deactivated glass liner. Generally, the internal standard concentration is held constant and the analyte concentration varied to establish a calibration curve, but to investigate the utility of 3,4-DNT as an internal standard the injection concentrations of 3,4-DNT and TNT (Table 1) are equal (Fig. 2). With the exception of the 50 mL min<sup>-1</sup> flow rate, 3,4-DNT peak areas overlap with the TNT peak areas within one standard deviation regardless of flow rate. This result suggests similar vaporization behavior of 3,4-DNT to TNT with a standard GC inlet at constant inlet temperature. The

relatively small differences in peak areas in Fig. 2 between 3,4-DNT and TNT can be attributed to differences in detection with a  $\mu$ ECD. It is plausible that the additional nitro group on the benzene ring for TNT increases its electron affinity compared to 3,4-DNT and the  $\mu$ ECD response is based on electron affinity. Consequently, TNT will have a slightly higher response than 3,4-DNT with a  $\mu$ ECD. More importantly, results in Fig. 2A illustrate the utility of 3,4-DNT as an internal standard because its behavior is consistent with that of TNT regardless of inlet flow rate (split ratio).

Conventionally, liquid samples are vaporized upon injection via contact with a heated glass liner in a standard GC inlet. Alternatively, analytes can be adsorbed, or trapped, on the surface of a cooled glass liner and then rapidly heated and vaporized in cryo-focusing configurations. In both configurations, surface effects must be minimized, especially for analytes with relatively high sticking coefficients such as nitroaromatics [24,25], to reduce carry over, and optimize detection limits. Coated glass liners are commercially available to reduce the surface affinity of analytes for glass and theoretically increase vaporization efficiency. The performance of a Siltek<sup>TM</sup>-coated glass liner was investigated and compared to a deactivated glass liner for both 3,4-DNT and TNT. The Siltek<sup>TM</sup>-coated glass liner was evaluated as a widely available liner with silanized surface passivation treatment. Fig. 2B shows the peak areas for 3,4-DNT and TNT using a standard GC inlet with liquid samples and a Siltek<sup>TM</sup>-coated liner. Again, the concentrations of 3,4-DNT and TNT are equal for comparison and to determine

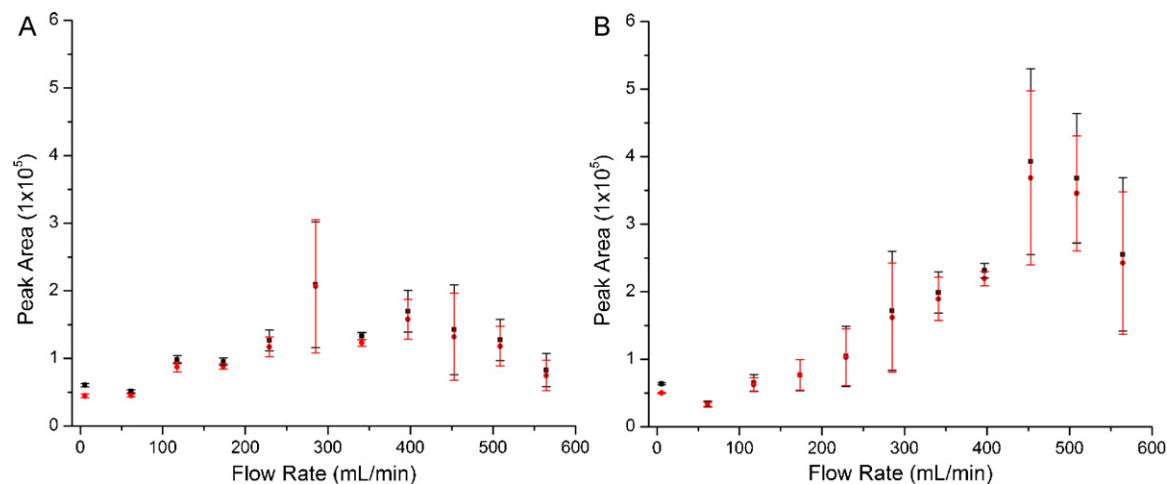


**Fig. 2.** The peak areas for 3,4-DNT and TNT at different flow rates through a standard split/splitless GC inlet with (A) a deactivated and (B) a Siltek<sup>TM</sup>-coated glass liner (■ = DNT; ● = TNT). Different flow rates were achieved by changing the split ratio; liquid sample concentrations were adjusted to maintain a consistent amount of analyte and internal standard on column. All error bars represent one standard deviation ( $N=3$ ).

differences in vaporization efficiency between the internal standard and the analyte of interest. The 3,4-DNT peak areas overlap within one standard deviation with the TNT peak areas and maintain a consistent ratio at flow rates greater than  $50 \text{ mL min}^{-1}$ , similar to the results in Fig. 2A with a deactivated glass liner. The comparison between the deactivated and Siltek<sup>TM</sup>-coated glass liners in Fig. 2 provides further evidence of the utility of 3,4-DNT as an internal standard since the liner treatment effects both compounds equally. The peak areas for both 3,4-DNT and TNT in Fig. 2B increase with increasing flow rate, yet the ratio of 3,4-DNT peak area to TNT peak area remains relatively constant. Both the 3,4-DNT and TNT peak areas increase with flow rate, which suggests a flow rate dependent phenomenon for vaporization of nitroaromatics with a Siltek<sup>TM</sup>-coated glass liner. However, normalizing against the 3,4-DNT internal standard, which maintains a consistent ratio to TNT regardless of flow rate, accounts for the observed flow rate dependence with a Siltek<sup>TM</sup>-coated glass liner.

### 3.2. Comparison between a CIS and standard GC inlet injections

For the quantitative measurement of TNT collected on a sampling tube, a CIS is used in conjunction with a TDS for sample injection. Therefore, an investigation on CIS liner treatment was conducted for deactivated and Siltek<sup>TM</sup>-coated glass liners with liquid sample injections into a CIS at various flow rates. The CIS temperature was held constant at  $250^\circ\text{C}$  with no cryo-focusing or temperature ramps to closely mimic a standard GC inlet. The liquid samples prepared according to Table 1 were designed to yield a 1:1 ratio of 3,4-DNT and TNT peak areas, assuming similar injection and detection behavior for both molecules. Thus, a normalized peak area of TNT to 3,4-DNT, assuming no losses and similar detector response, should be near unity. Fig. 3 shows the normalized peak area for TNT as a function of inlet flow rate for a standard split/splitless inlet and CIS with a deactivated (Fig. 3A) and a Siltek<sup>TM</sup>-coated (Fig. 3B) glass liner. The CIS and standard GC inlet yield surprisingly different results for TNT with a deactivated glass liner. Both inlets show flow rate dependence with a larger deviation from unity below  $100 \text{ mL min}^{-1}$  in Fig. 3A, but as the inlet flow rate increases, the CIS appears to approach unity while the standard GC inlet deviates. The results are different when the deactivated glass liner is replaced with a Siltek<sup>TM</sup>-coated glass liner (Fig. 3B). At flow rates greater than  $100 \text{ mL min}^{-1}$ , the normalized peak areas for a CIS injection overlap within one standard deviation of the normalized peak areas for a standard GC inlet. These data demonstrate the CIS and standard GC inlet vaporize TNT and 3,4-DNT similarly when a Siltek<sup>TM</sup>-coated glass liner is used. Differences in 3,4-DNT and TNT vaporization between the two inlets are more dramatic with a deactivated glass liner. Thus, a Siltek<sup>TM</sup>-coated liner should be used to obtain quantitative information about TNT, especially when using a CIS for sample introduction and a standard GC inlet for establishing calibration curves from standard solutions.

A flow rate dependence for both 3,4-DNT and TNT is observed in Figs. 2 and 3. In Fig. 2B, the peak areas for 3,4-DNT and TNT increase with flow rate, but because peak areas increase similarly for both molecules, this trend is mitigated through normalization. Regardless of liner treatment and inlet configuration, statistical differences appear at flow rates below  $50 \text{ mL min}^{-1}$ . The 3,4-DNT peak areas are statistically different from TNT at flow rates less than  $50 \text{ mL min}^{-1}$  according to Fig. 2, and the differences are further exemplified in the normalized peak areas of Fig. 3 with a large deviation from unity with either a deactivated or Siltek<sup>TM</sup>-coated glass liner. Below  $200 \text{ mL min}^{-1}$  in Fig. 3B the standard deviations are relatively larger, suggesting inconsistent vaporization. When the flow rate is increased above  $200 \text{ mL min}^{-1}$ , the CIS and standard GC inlet behave almost identical with a Siltek<sup>TM</sup>-coated glass liner. These results indicate a minimum inlet flow rate of  $200 \text{ mL min}^{-1}$

should be used for quantitative detection of TNT when using liquid sample calibration curves and vapor sampled analytes. A flow rate of  $200 \text{ mL min}^{-1}$  through the CIS for injections is consistent with previous literature [18].

### 3.3. Effects of initial inlet temperature and ramping for a CIS injection

The CIS parameters were optimized with liquid injections for eventual addition of the TDS. Analyte was cryo-focused on the CIS inlet before the temperature was ramped to desorb, vaporize, and inject analyte onto the GC column. The CIS temperature ramp was held constant at  $12^\circ\text{C s}^{-1}$ , while the initial inlet temperature was investigated. Based on the results from the previous section, a Siltek<sup>TM</sup>-coated glass liner was used for CIS optimization while operated in split mode. Fig. 4 shows the peak areas for 3,4-DNT and TNT at three different initial inlet temperatures:  $-50^\circ\text{C}$  (Fig. 4A),  $0^\circ\text{C}$  (Fig. 4B), and  $50^\circ\text{C}$  (Fig. 4C). Each injection was done in triplicate and the error bars represent one standard deviation. A trend is observed with all three initial inlet temperatures where a plateau is reached in peak areas for both 3,4-DNT and TNT at flow rates greater than  $200 \text{ mL min}^{-1}$ . The peak areas for both 3,4-DNT and TNT decrease significantly at flow rates less than  $200 \text{ mL min}^{-1}$  for  $0^\circ\text{C}$  and  $50^\circ\text{C}$  initial inlet temperatures. Response for the two nitroaromatics deviates below  $200 \text{ mL min}^{-1}$  at an initial inlet temperature of  $-50^\circ\text{C}$  (Fig. 4A). A minimum flow rate is necessary for efficient desorption of nitroaromatics from the Siltek<sup>TM</sup>-coated glass liner surface in a cryo-focusing configuration. For all three initial inlet temperatures, a stable, consistent response for 3,4-DNT and TNT is achieved at  $200 \text{ mL min}^{-1}$  with no significant improvement at higher flow rates. This result is further evidence of a flow rate dependent vaporization mechanism within the CIS for nitroaromatics.

It is difficult to determine the optimal initial inlet temperature for nitroaromatics from peak area alone. To help determine the optimal initial inlet temperature, Fig. 4D shows the peak area of TNT normalized to 3,4-DNT for all three initial inlet temperatures. The 3,4-DNT and TNT samples were prepared to yield an equivalent on-column injection load, and a normalized peak area of unity would indicate no losses. The plateau observed at flow rates greater than  $200 \text{ mL min}^{-1}$  is also observed in the normalized peak area of Fig. 4D. The normalized peak area for all three initial inlet temperatures approach unity as the flow rate increases. Furthermore, the CIS injections with cryo-focusing show a notable improvement in reproducibility over a standard GC inlet based on the standard deviations (error bars) at each flow rate, especially for the initial inlet temperature of  $0^\circ\text{C}$  (●). Based on the magnitude of the error bars in Fig. 4D, an initial inlet temperature of  $0^\circ\text{C}$  provided the most consistent, reproducible quantitative information for TNT. An initial inlet temperature of  $-50^\circ\text{C}$  is also reasonable from a reproducibility view, but from a practical view initial inlet temperature of  $0^\circ\text{C}$  reduces liquid nitrogen consumption and decreases run times, as long as an inlet flow rate greater than  $200 \text{ mL min}^{-1}$  is used.

### 3.4. Effect of solvent vent mode CIS injections

A splitless injection often provides improved detection limits and is necessary for trace analysis, but split inlet flow provides improved inlet flow stability and extends the high end of the GC linear dynamic range by reducing the solvent load. As with conventional GC inlets, the CIS offers a solvent vent mode for trapping the desired, less volatile analytes on the cooled liner while purging solvent from the liner at an increased flow rate for a user defined vent time, either before or during the CIS temperature ramp. Solvent vent mode is the manufacturer-recommended mode for trace

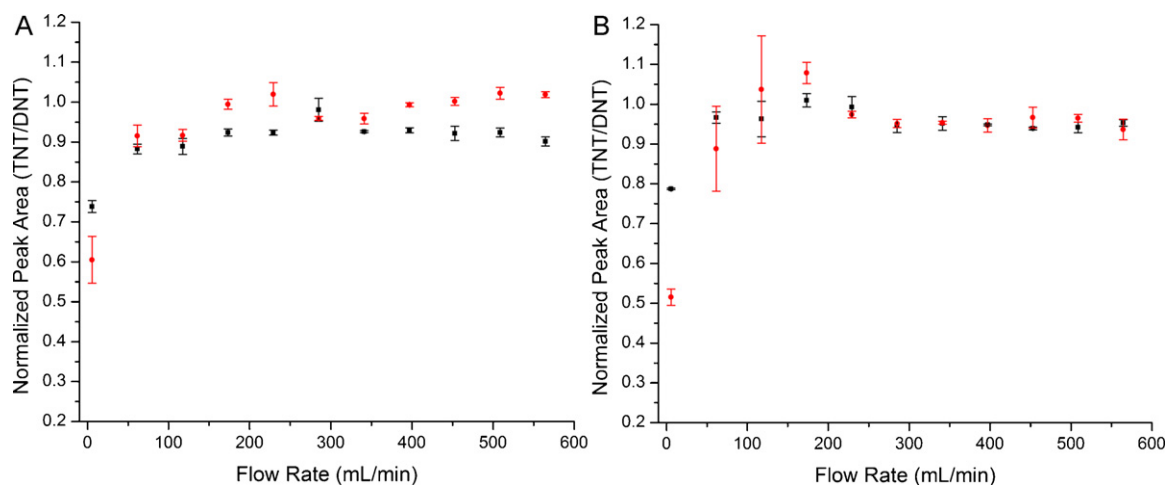


**Fig. 3.** The normalized peak area for TNT with 3,4-DNT as an internal standard using a (■) standard split/splitless GC inlet and a (●) CIS operated at a constant 250 °C with a (A) deactivated and (B) Siltek™-coated glass liner. The error bars represent one standard deviation at the various inlet flow rates ( $N=3$ ).

analysis when coupled to the TDS. However, one must minimize analyte loss during the TDS desorption and CIS trapping process. The fast CIS temperature ramp is on the order of seconds ( $12^{\circ}\text{C s}^{-1}$ ) to provide a sharp injection of analyte onto the GC column.

In contrast, the TDS desorption is relatively long, taking ca. 7.5 min, while the CIS desorption cycle takes ca. 25 s. In this context, the stability of 3,4-DNT and TNT during the long TDS desorption cycle needs to be characterized.

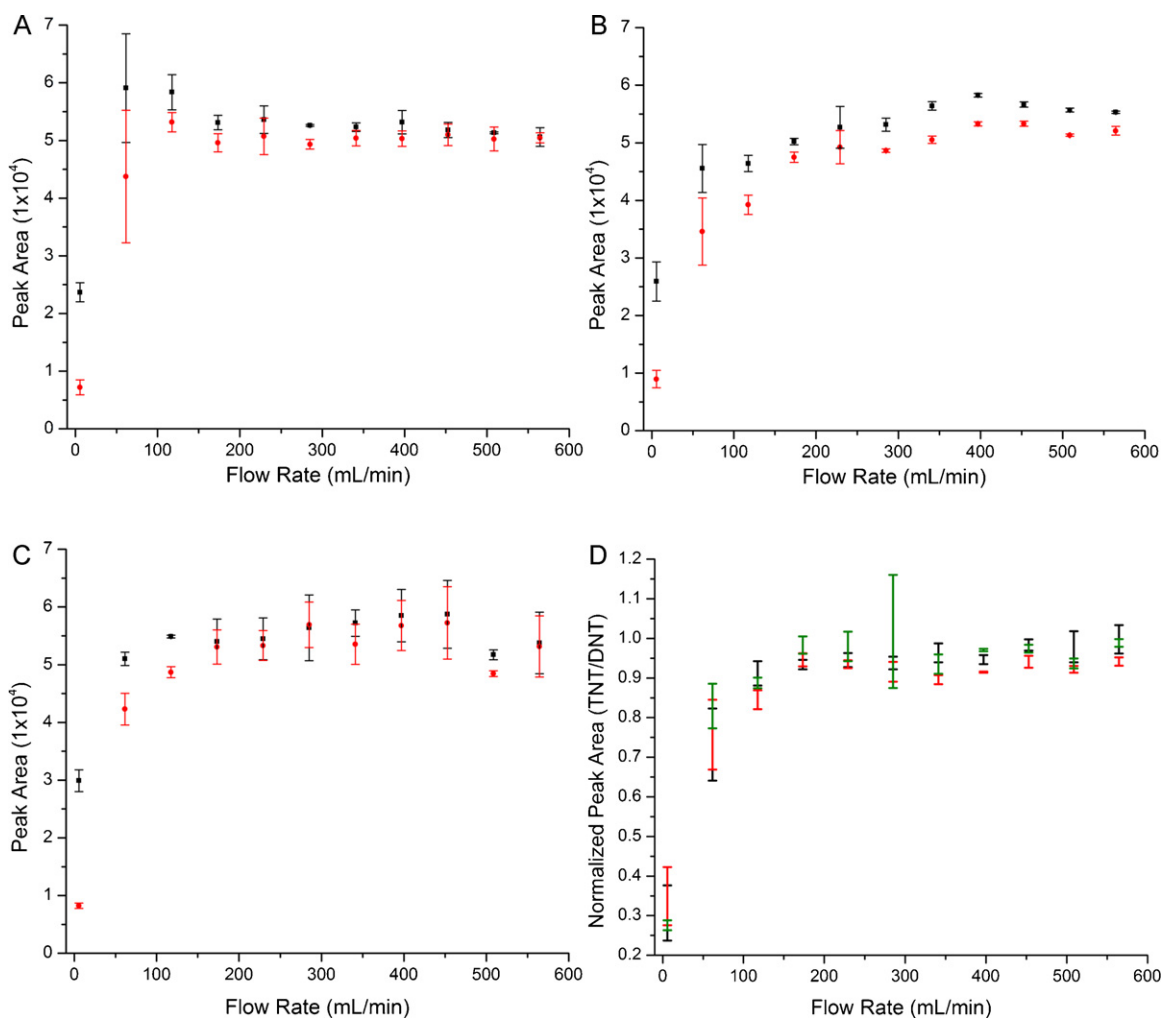


**Fig. 4.** The peak areas for (■) 3,4-DNT and (●) TNT using a CIS with a Siltek™-coated glass liner and liquid samples at (A) -50 °C, (B) 0 °C, and (C) 50 °C initial inlet temperature. (D) The normalized peak areas for TNT at various inlet flow rates for three initial inlet temperatures (black = -50 °C; red = 0 °C; green = 50 °C). The symbols have been eliminated for clarity but lie within the median of the error bars. Error bars represent one standard deviation ( $N=3$ ).



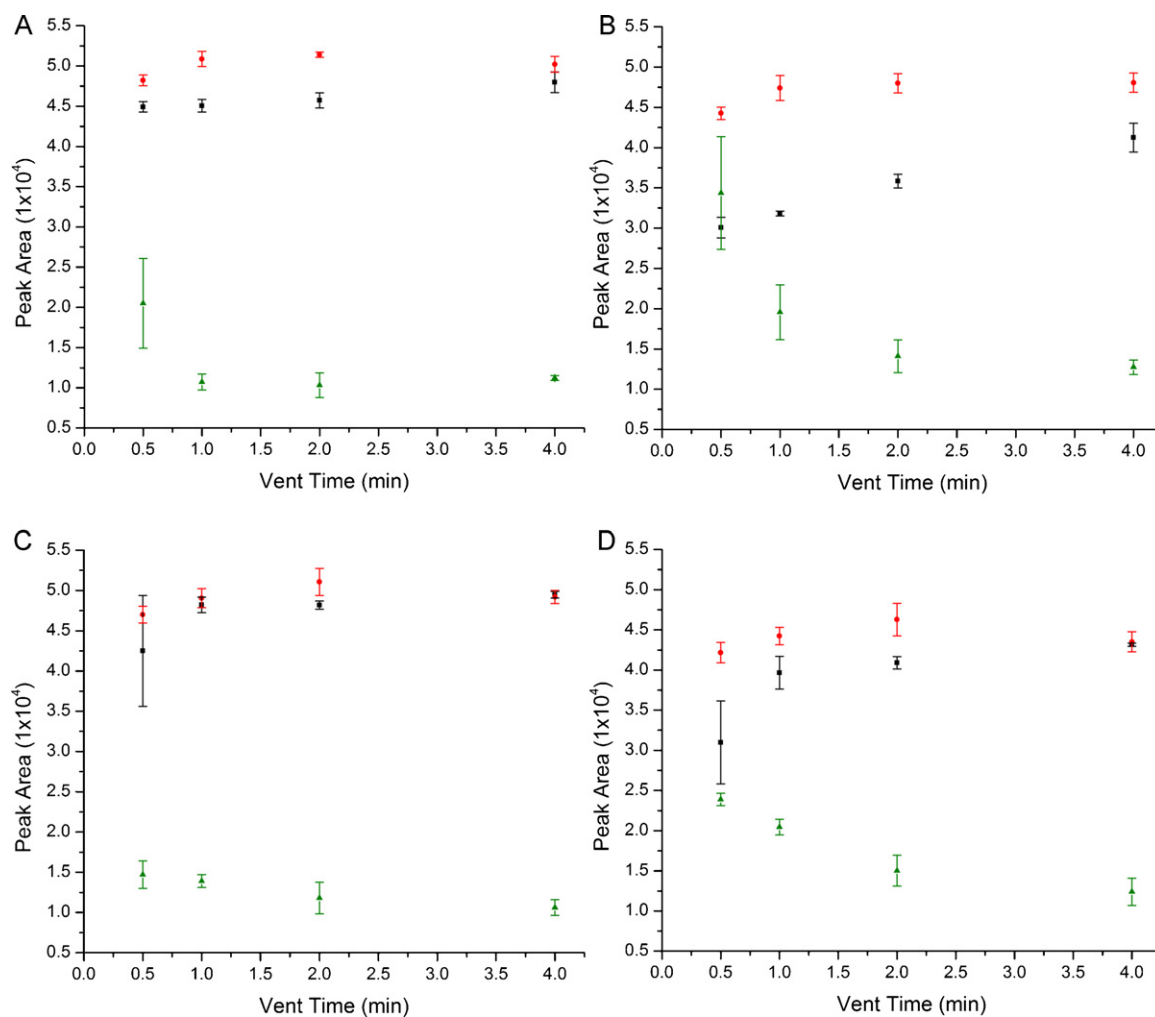


**Fig. 5.** The peak areas for (A) 3,4-DNT and (B) TNT at 285 mL min<sup>-1</sup> and (C) 3,4-DNT and (D) TNT at 580 mL min<sup>-1</sup> inlet flow rate using a CIS with different vent times. The injections were conducted at three different initial inlet temperatures: (■) -50 °C, (●) 0 °C, and (▲) 50 °C in triplicate with error bars representing one standard deviation ( $N=3$ ).

The vent time parameter was investigated at various inlet flow rates and initial inlet temperatures using liquid injections onto the CIS, prior to TDS coupling. Fig. 1A shows the timing of the solvent vent mode: the vent state, the CIS temperature ramp, and GC oven temperature profile. The vent time occurs before the start of the CIS temperature ramp to improve retention of less volatile analytes. Fig. 5 shows the peak areas for 3,4-DNT and TNT at two different inlet flow rates (285 and 580 mL min<sup>-1</sup>) and three initial inlet temperatures. Three replicate measurements were made under each set of conditions and error bars represent one standard deviation. Flow rates less than 285 mL min<sup>-1</sup> were not investigated based on the results from Fig. 4. Unlike the split injection, where the initial inlet temperature had little to no effect on peak area at flow rates greater than 200 mL min<sup>-1</sup>, the initial inlet temperature for the solvent vent mode is important, regardless of flow rate. The peak area for 3,4-DNT is significantly lower at an initial inlet temperature of 50 °C. The 3,4-DNT is less effectively adsorbed in the CIS at 50 °C. Consequently, not all of the 3,4-DNT is trapped at 50 °C (Fig. 5A), and this effect is exacerbated at higher flow rates (Fig. 5C). The ineffective trapping at initial inlet temperatures greater than 0 °C is also observed for TNT. In Fig. 5B and D, the peak areas for TNT decrease with an increase in vent time at an initial inlet temperature of 50 °C. This result demonstrates that TNT is ineffectively adsorbed onto the Siltek<sup>TM</sup>-coated glass liner at an elevated temperature and consequently, TNT is vented instead of trapped for

trace analysis. Regardless of flow rate, peak areas for 3,4-DNT and TNT are maximized at 0 °C, except for 3,4-DNT at 580 mL min<sup>-1</sup> flow rate (Fig. 5C), where there is no significant difference in peak area at either -50 °C or 0 °C. Therefore, an initial inlet temperature of 0 °C can be used in combination with a solvent vent. This result is consistent with the optimized conditions for liquid injections with a CIS operated in split mode.

The optimal initial inlet temperature for the CIS solvent mode to minimize analyte loss has been established as 0 °C, but an appropriate vent time must also be determined. The peak areas for both 3,4-DNT and TNT appear to reach a maximum with a 2.0 min vent time for a 0 °C initial inlet temperature in Fig. 5. The 2.0 min vent time at 0 °C is also optimal regardless of flow rate through the inlet. This is an important characteristic because a flow rate dependence has been observed for 3,4-DNT and TNT adsorption/desorption and higher flow rates might be necessary to effectively desorb these analytes from sampling tubes with the TDS. Thus, a 2.0 min vent time and a 0 °C initial inlet temperature are optimal for trace quantitative analysis of TNT using a CIS in solvent vent mode.

### 3.5. Injection via TDS–CIS system

The TDS was attached after characterizing the CIS with liquid samples and the SLH. A temperature ramp profile from 25 °C to 250 °C at 40 °C min<sup>-1</sup> with a 2.0 min hold time at 250 °C was used.

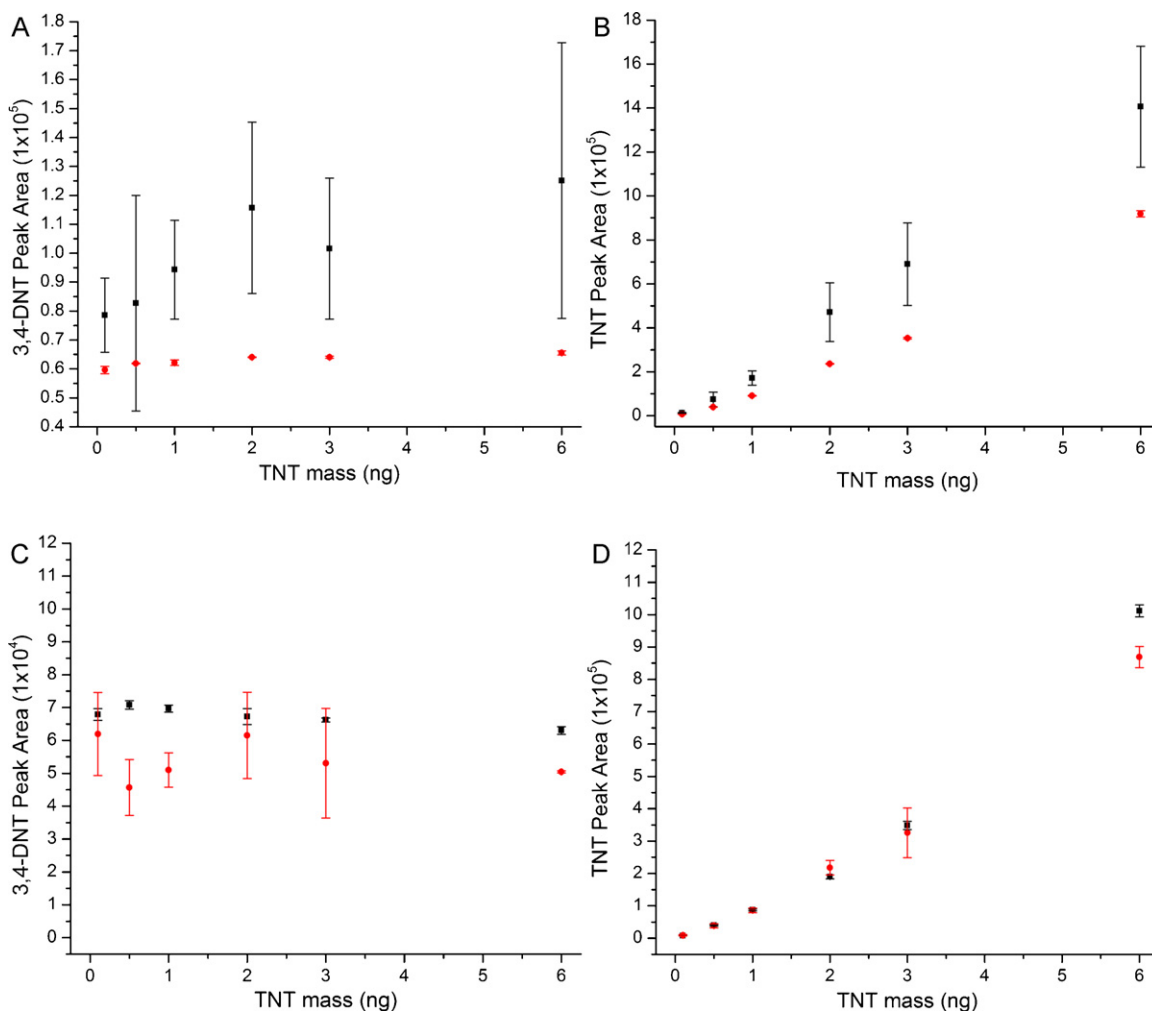


**Fig. 6.** Plot of peak area versus mass for (A) 3,4-DNT and (B) TNT using (■) a standard GC inlet and (●) an optimized CIS with cryo-focusing enabled. Similarly, the peak area versus TNT standard mass for (C) 3,4-DNT and (D) TNT using (■) a Tenax<sup>®</sup>-filled and (●) empty sample tube with standard solutions injected directly onto the frit of both types of vapor sample tubes. The error bars for all plots represent one standard deviation ( $N=3$ ). The 3,4-DNT mass was held constant for all masses of TNT since it is utilized as an internal standard. These plots are then used to establish calibration curves of the normalized peak area (TNT/3,4-DNT).

A flow rate of  $285 \text{ mL min}^{-1}$  through the TDS during desorption was selected based on the results from the previous experiments, where a flow rate dependence was observed and at least  $200 \text{ mL min}^{-1}$  was necessary for reproducible desorption of both 3,4-DNT and TNT (Fig. 4D). Liquid samples were deposited onto either Tenax<sup>®</sup> 60/80 filled or empty vapor sampling tubes, and the solvent (acetonitrile) was allowed to evaporate for at least 20 min. The hold time was extended to 4.0 min with no significant change in peak areas for either 3,4-DNT and TNT. These conditions are consistent with previous literature, which also used a  $285 \text{ mL min}^{-1}$  flow rate for in-port desorption of TNT from a plastic wipe [18].

Calibration curves were established for standard solutions using a standard GC inlet and a CIS optimized method. Fig. 6A shows peak area versus mass for 3,4-DNT with a standard GC inlet and a CIS. Calibration curves are generally established using an internal standard at a constant concentration or mass; hence, the 3,4-DNT mass has been held constant. Ideally, a plot of 3,4-DNT peak area for each mass of TNT would yield a horizontal line. This is not true for the standard GC inlet in Fig. 6A. The error bars, a representation of the variability associated with the inlet, injection, and method, for the standard GC inlet are relatively large compared to the error bars for 3,4-DNT using a CIS. However, the overall magnitude of the 3,4-DNT peak areas has decreased significantly, within one standard deviation, relative to the peak areas for a standard GC inlet.

Despite the use of an optimized method, there is some significant loss of 3,4-DNT with a CIS injection using standard solutions, but the reproducibility is improved.

The peak area for TNT at different TNT masses spread across the entire dynamic range of the  $\mu\text{ECD}$  is seen in Fig. 6B. Similar to the results with 3,4-DNT using the optimized CIS injection method with temperature ramping, the magnitude of the TNT peak area is statistically less within one standard deviation for the CIS versus a standard GC inlet, but the error bars are noticeably improved. Again, the optimized CIS method yields more reproducible results for nitroaromatics, but there is a loss of both analyte and internal standard. The source of the loss is not known, but it is likely due to poor trapping efficiency in the CIS liner. Adjustment of the temperature ramp delay relative to the vent time may yield more insight into the source of the loss between the CIS and a standard GC inlet. Despite this loss, calibration curves can reliably be established with a CIS and standard solution injections.

The direct deposition of standard solutions on a vapor sampling tube for quantitation was evaluated by establishing a calibration curve for 3,4-DNT and TNT using a TDS-CIS with the optimized CIS method. Liquid deposits were placed in both Tenax<sup>®</sup>-filled and empty sample tubes. Fig. 6C shows the peak area of the internal standard, 3,4-DNT, at different TNT masses for the two types of vapor sampling tubes. The 3,4-DNT peak area is most constant

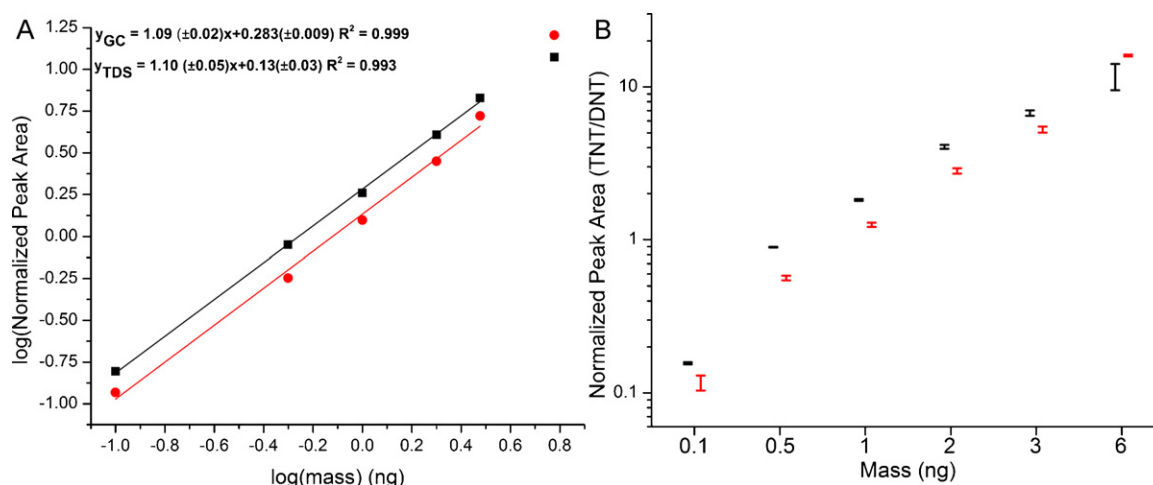


**Fig. 7.** (A) Calibration curves for liquid samples with (■) a standard split/splitless GC inlet and (●) a TDS–CIS using Tenax<sup>®</sup>-filled sample tubes with direct liquid deposition. All samples were run in triplicate, but errors bars are not visible with the log–log scale. The slopes, intercepts, and  $R^2$  values for the calibration curves for the standard GC inlet ( $y_{GC}$ ) and TDS–CIS ( $y_{TDS}$ ) are also displayed, respectively. (B) The error, one standard deviation, for each injection method for three replicate injections. The colors match the calibration curve and are plotted left-to-right per mass of TNT: standard split/splitless GC inlet and a TDS–CIS using Tenax<sup>®</sup>-filled sample tubes with direct liquid deposition.

across TNT masses for sample tubes filled with Tenax<sup>®</sup>, as indicated by the relatively small error bars and consistent peak areas shown in Fig. 6C. The empty sample tubes yield a decrease in reproducibility indicated by the relatively large error bars (one standard deviation) compared to the Tenax<sup>®</sup>-filled tubes. It is believed the source of the increased variability for 3,4-DNT using empty tubes is related to the gas temperature through the sample tube and flow dynamics. The gas flowing through the Tenax<sup>®</sup>-filled sample tube passes over more heated surface area via a packed sorbent bed. The empty sample tube only provides the gas molecules closest to the walls reaching the maximum desorption temperature (250 °C) before passing through the glass frit of the sample tube. This is similar to the results observed with the initial inlet temperature and CIS temperature ramp, where 3,4-DNT was more efficiently desorbed with a higher temperature inlet. Furthermore, the relatively small volumes of liquid (5  $\mu$ L) used for direct liquid deposition do not carry the liquid samples into the Tenax<sup>®</sup> layer, but merely distribute it on the glass frit. Thus, the difference between the Tenax<sup>®</sup>-filled and empty sample tube calibration curves for 3,4-DNT is not a difference in desorption between Tenax<sup>®</sup> and glass, but more likely related to flow dynamics and heat. The exact cause of the increased variability associated with the direct liquid deposition method onto empty sample tubes is not fully understood, but it is recommended to use the Tenax<sup>®</sup>-filled sample tubes to yield more reproducible and consistent results for nitroaromatics.

The TNT peak area in Fig. 6D does not appear to be effected by the sample tube construction (empty or Tenax<sup>®</sup>-filled). At masses less than 3 ng, there is no statistical difference in TNT peak area between a Tenax<sup>®</sup>-filled or empty sample tube. As the mass reaches 3 ng and greater, the error bars for TNT peak area increase for an empty sample tube, suggesting that due to the lower gas temperature, there is variable desorption of TNT from the glass frit of the sample tube. Similar to 3,4-DNT, a packed, Tenax<sup>®</sup>-filled sample tube should be used in association with the direct liquid deposition method for establishing calibration curves of nitroaromatics. Of note, the larger error bars for 6 ng of TNT (Fig. 6A and B) are at the maximum of the  $\mu$ ECD's dynamic range. The detector becomes saturated at approximately 5.5 ng of TNT and the variability observed at 6 ng is associated with detector saturation.

Calibration curves are typically established with the normalized peak area of the analyte of interest versus an internal standard. Fig. 7A shows a calibration curve with the normalized peak area for TNT on a log–log scale with 3,4-DNT as the internal standard at

constant mass for a standard GC inlet and the direct liquid deposition method using a TDS–CIS inlet. Error bars have been omitted for clarity and are instead shown in Fig. 7B, which is a representation of the error for each mass used in the calibration curves for each sample introduction method. The error bars are horizontally offset for clarity. The normalized peak area for TNT at 6 ng has been excluded from the linear fit in Fig. 7A because it is beyond the dynamic range of the detector. The equation of the lines along with the coefficient of determination ( $R^2$ ) for the two linear fits are shown in Fig. 7A as  $y_{GC}$  and  $y_{TDS}$  for the calibration curve for the standard GC inlet and the TDS–CIS, respectively. As expected, the standard GC inlet yields a relatively linear calibration curve on a log–log scale with a  $R^2$  near unity. The TDS–CIS calibration curve with direct liquid deposition method has a nearly identical slope to the standard GC inlet calibration curve within one standard deviation, but the  $R^2$  deviates from unity. The nearly identical slope between the two calibration curves indicates that the direct liquid deposition method can be used for establishing calibration curves, but there is an inherent loss associated with the TDS–CIS injection. The loss is relatively consistent and independent of TNT mass, as is demonstrated in Fig. 7A. The source of the loss is not known, but it is believed to be related to the desorption process within the TDS and compounded by the loss observed for the CIS in Fig. 6B for TNT. The offset and associated loss with the TDS does not preclude the use of the direct liquid deposition process for establishing calibration curves, but does indicate routine liquid sample injections should be performed to ensure the offset remains constant, and apply appropriate correction when obtaining quantitative information about vapor samples collected on Tenax<sup>®</sup>-filled sample tubes. While quantitation of TNT vapor samples using the direct liquid deposition method has not been presented, the losses associated with the instrumentation and the viability of the direct liquid deposition method for explosive vapor quantitation has been demonstrated.

#### 4. Conclusions

A new simple direct liquid deposition method for establishing calibration curves for explosives from vapor sample tubes was compared to liquid injections on a standard split/splitless GC inlet. To evaluate the utility of the direct liquid deposition method, losses associated with each component of the TDS–CIS system were characterized relative to a standard split/splitless GC inlet, and 3,4-DNT was introduced as an internal standard. It was determined that inlet



flow rates above 200 mL min<sup>-1</sup> are required for the CIS to perform comparably to a standard GC inlet. Furthermore, there was a flow rate dependent desorption of 3,4-DNT and TNT from both a deactivated and Siltek<sup>TM</sup>-coated glass liner. The use of a Siltek<sup>TM</sup>-coated glass liner, a flow rate of 285 mL min<sup>-1</sup>, an initial inlet temperature of 0 °C, and a solvent vent time of 2.0 min were optimal for quantitative analysis of TNT using a CIS for both liquid samples and vapors introduced from a TDS. These results are consistent with previous investigations for the operation of individual components but until now has not been evaluated from a complete systems view for a TDS–CIS–GC–ECD. Calibration curves were established for a standard GC inlet and TDS–CIS configurations with liquid samples and directly depositing standard solutions onto Tenax<sup>®</sup>-filled and empty sample tubes. Comparison of Tenax<sup>®</sup>-filled to empty sample tubes using the direct liquid deposition method indicated heating and a flow dynamic dependence for reproducible desorption of 3,4-DNT and TNT. The Tenax<sup>®</sup>-filled sample tubes yielded more consistent results. An offset between the standard GC inlet and Tenax<sup>®</sup>-filled direct liquid deposition calibration curves indicated a loss associated with the TDS–CIS, but the loss was independent of TNT mass. Most importantly, the linear response and improved reproducibility for the direct liquid deposition method demonstrates its significant advantage over traditional methods for quantitation of explosive vapors.

#### Acknowledgements

The authors would like to acknowledge Mark Hammond for his help in generating figures. Financial support was provided by the Department of Homeland Security Science and Technology Directorate.

#### References

- [1] J. Yinon, S. Zitrin, *Modern Methods and Applications in Analysis of Explosives*, John Wiley & Sons, Ltd., West Sussex, 1993.
- [2] D. Collins, M. Lee, *Anal. Bioanal. Chem.* 372 (2002) 66.
- [3] G.A. Eiceman, D. Preston, G. Tian, J. Rodriguez, J.E. Parmeter, *Talanta* 45 (1997) 57.
- [4] P.-C. Chen, S. Sukcharoenchoke, K. Ryu, L.G. de Arco, A. Badmaev, C. Wang, C. Zhou, *Adv. Mater.* 22 (2010) 1900.
- [5] M.B. Pushkarsky, I.G. Dunayevskiy, M. Prasanna, A.G. Tsekoun, R. Go, C.K.N. Patel, *Proc. Natl. Acad. Sci. U. S. A.* 103 (2006) 19630.
- [6] J. Yinon, *Anal. Chem.* 75 (2003) 98A.
- [7] D.S. Moore, *Rev. Sci. Instrum.* 75 (2004) 2499.
- [8] K.J. Albert, D.R. Walt, *Anal. Chem.* 72 (2000) 1947.
- [9] J.M.F. Douse, *J. Chromatogr.* 234 (1982) 415.
- [10] M.E. Sigman, C.-Y. Ma, *J. Forensic Sci.* 46 (2001) 6.
- [11] M.E. Walsh, *Talanta* 54 (2001) 427.
- [12] M.E. Sigman, C.-Y. Ma, R.H. Ilgner, *Anal. Chem.* 73 (2001) 792.
- [13] M. Hable, C. Stern, C. Asowata, K. Williams, *J. Chromatogr. Sci.* 29 (1991) 131.
- [14] F. Belkin, R.W. Bishop, M.V. Sheely, *J. Chromatogr. Sci.* 23 (1985) 532.
- [15] J. Yinon, *J. Chromatogr. A* 742 (1996) 205.
- [16] J.M.F. Douse, *J. Chromatogr.* 208 (1981) 83.
- [17] M.E. Sigman, C.-Y. Ma, *Anal. Chem.* 71 (1999) 4119.
- [18] R. Waddell, D.E. Dale, M. Monagle, S.A. Smith, *J. Chromatogr. A* 1062 (2005) 125.
- [19] E. Psillakis, N. Kalogerakis, *J. Chromatogr. A* 907 (2001) 211.
- [20] M. Kirchner, E. Matisova, S. Hrouzkova, R. Huskova, *Pet. Coal* 49 (2007) 72.
- [21] US Environmental Protection Agency Method 529, Determination of Explosives and Related Compounds in Drinking Water by Solid Phase Extraction and Capillary Column Gas Chromatography/Mass Spectrometry (GC/MS). <http://www.epa.gov> (accessed May 2011).
- [22] US Environmental Protection Agency Method 8091, Nitroaromatics and Cyclic Ketones by Gas Chromatography. <http://www.epa.gov> (accessed May 2011).
- [23] US Environmental Protection Agency Method 8095, Explosives by Gas Chromatography. <http://www.epa.gov> (accessed May 2011).
- [24] G. Muralidharan, A. Wig, L.A. Pinnaduwaage, D. Hedden, T. Thundat, R.T. Lareau, *Ultramicroscopy* 97 (2003) 433.
- [25] L.A. Pinnaduwaage, D. Yi, F. Tian, T. Thundat, R.T. Lareau, *Langmuir* 20 (2004) 2690.